Data in brief 27 (2019) 104741

Contents lists available at ScienceDirect

Data in brief

journal homepage: www.elsevier.com/locate/dib

Data Article

Data in brief on CO_2 absorption-desorption of aqueous-based amino acid solvents with phase change behaviour

Masood S. Alivand [a, b], Omid Mazaheri [a, c], Yue Wu [a, b], Geoffrey W. Stevens [a, b], Colin A. Scholes [a, b], Kathryn A. Mumford [a, b, *]

[a] Department of Chemical Engineering, The University of Melbourne, Parkville, Victoria, 3010, Australia
[b] Peter Cook Centre for CCS Research, The University of Melbourne, Parkville, Victoria, 3010, Australia
[c] School of Agriculture and Food, Faculty of Veterinary and Agricultural Sciences, The University of Melbourne, Parkville, Victoria, 3010, Australia

ARTICLE INFO

Article history:
Received 7 October 2019
Accepted 28 October 2019
Available online 4 November 2019

Keywords:
Amino acid
Phase change solvent
Anti-solvent
CO_2 absorption
Energy-efficiency

ABSTRACT

The data presented in this paper are related to the published research article "Development of aqueous-based phase change amino acid solvents for energy-efficient CO_2 capture: The role of antisolvent" [1]. The raw and analyzed data include the equilibrium and kinetics of CO_2 absorption, the density and concentration of different CO_2-containing species at upper and lower liquid phases, and particle size distribution of solid particles precipitated during CO_2 absorption of aqueous and aqueous-based amino acid solvents. In addition, the SEM images of solid precipitates at the end of CO_2 absorption are presented. The detailed values of this phase change amino acid solvent are crucial for large-scale implementation of CO_2 capture systems with phase change behavior.

* Corresponding author. Department of Chemical Engineering, The University of Melbourne, Parkville, Victoria, 3010, Australia.
E-mail address: mumfordk@unimelb.edu.au (K.A. Mumford).

https://doi.org/10.1016/j.dib.2019.104741

Specifications Table

Subject	Energy and environmental engineering
Specific subject area	Phase separation and precipitation analysis
Type of data	Text Table Figure Image
How data were acquired	Equilibrium CO_2 absorption test rig Dynamic CO_2 absorption-desorption test rig Focused Beam Reflectance Measurement (FBRM) probe (ParticleTrack G400, Mettler Toledo) SEM (FlexSem 1000, Hitachi)
Data format	Raw and analyzed data
Parameters for data collection	The aqueous-based amino acid solvent was prepared at different volume ratios of DMF as anti-solvent
Description of data collection	Herein, the data was collected using equilibrium and dynamic CO_2 capture rigs. For equilibrium CO_2 absorption rig, pure CO_2 with a known initial pressure was injected into the solvent and final equilibrium pressure was recorded. For dynamic CO_2 absorption-desorption rig, a mixture of N_2 and CO_2 was injected into the solvent at a constant flow rate and the concentration of CO_2 was monitored at both inlet and outlet streams. Moreover, the solid particle precipitation was recorded during dynamic CO_2 absorption.
Data source location	Department of Chemical Engineering, The University of Melbourne, Parkville, Victoria 3010, Australia.
Data accessibility	Data is available in this article
Related research article	M.S. Alivand, O. Mazaheri, Y. Wu, G.W. Stevens, C.A. Scholes, K.A. Mumford, Development of aqueous-based phase change amino acid solvents for energy-efficient CO_2 capture: The role of antisolvent, Appl. Energ. 256 (2019) 113911. https://doi.org/10.1016/j.apenergy.2019.113911

Value of the Data

- The dataset can be used in future studies and analysis of phase change solvents with new amino acids and anti-solvents.
- These data will be crucial for researchers and engineers to design/improve large-scale phase change amino acid solvents with high energy-efficiency.
- It provides a new insight into the role of anti-solvent in phase change amino acid solvents and can be effectively employed in future works to find appropriate anti-solvents.
- This dataset can be used for other similar systems and provide applicable information for large-scale implementation of energy-efficient CO_2 capture systems.

1. Data

The data presented in this article are associated with the research article (M.S. Alivand et al., 2019 [1]) which were acquired using CO_2 absorption-desorption rigs of the University of Melbourne. Fig. 1 shows the CO_2 absorption-desorption rig for measuring dynamic CO_2 absorption capacity, monitoring solid particle precipitation and highly-accurate heat transfer calorimetry analysis. Fig. 2a and b shows the effect of potassium hydroxide (KOH)/potassium glycinate (GlyK) ratio on the pH value and dynamic CO_2 absorption capacity of aqueous 3 M potassium glycinate solvent at 40 °C, respectively. Figs. 3 and 4 demonstrate the number of precipitated solid particles and particle size distribution for different initial GlyK and anti-solvent concentrations during dynamic CO_2 absorption. The density, CO_2 absorption capacity, carbamate and carbonate/bicarbonate concentration of prepared aqueous and aqueous-based GlyK solvents are presented in Tables 1 and 2. The spontaneous liquid-liquid phase separation of aqueous-based GlyK-70 and GlyK-80 solvents before CO_2 absorption is illustrated in Fig. 5. Fig. 6 shows the SEM images of solid precipitated particles at the end of CO_2 absorption for aqueous-based GlyK-55, GlyK-60 and GlyK-65 solvents.

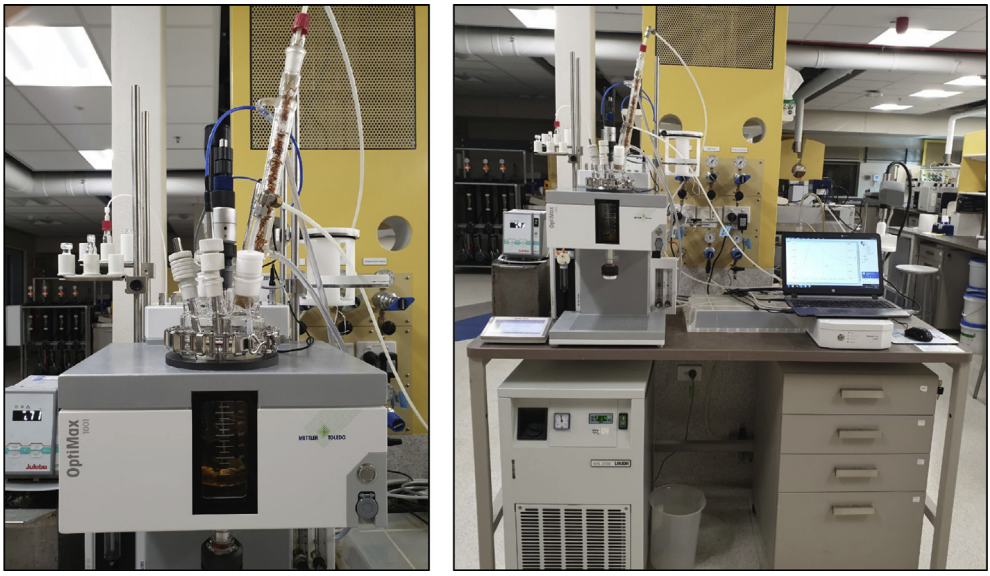

Fig. 1. Dynamic CO_2 absorption-desorption rig equipped with Focused Beam Reflectance Measurement (FBRM) probe for online monitoring solid precipitation and HFCal probe for quantitative heat flow calorimetry analysis.

2. Experimental design, materials, and methods

2.1. Dynamic CO_2 absorption/desorption experiments

The rate of dynamic CO_2 absorption in the loaded solution can be computed by the total mass balance of CO_2:

$$Q_{CO_2} = n^{in}_{CO_2} - n^{out}_{CO_2} \tag{1}$$

where Q_{CO_2} is the rate of CO_2 absorption; $n^{in}_{CO_2}$ is the CO_2 molar flowrate at inlet stream; $n^{out}_{CO_2}$ is the CO_2 molar flowrate at outlet stream.

The recorded CO_2 concentration at outlet streams can be defined as:

$$x^{out}_{CO_2} = \frac{n^{out}_{CO_2}}{n^{out}_{CO_2} + n^{out}_{N_2}} \tag{2}$$

where $x^{out}_{CO_2}$ is the volume fraction of CO_2 at outlet stream; $n^{out}_{N_2}$ is the N_2 flowrate at outlet stream. Equation (2) can be represented by:

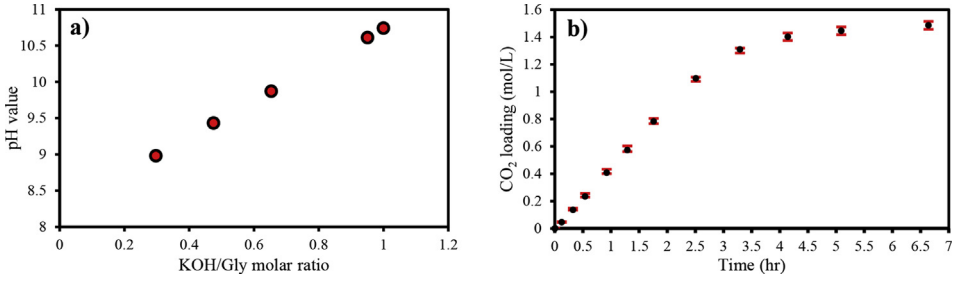

Fig. 2. (a) pH value of potassium glycinate solution at different KOH/Gly molar ratios and (b) dynamic CO_2 absorption capacity of aqueous 3 M GlyK-0 solvent at 40 °C.

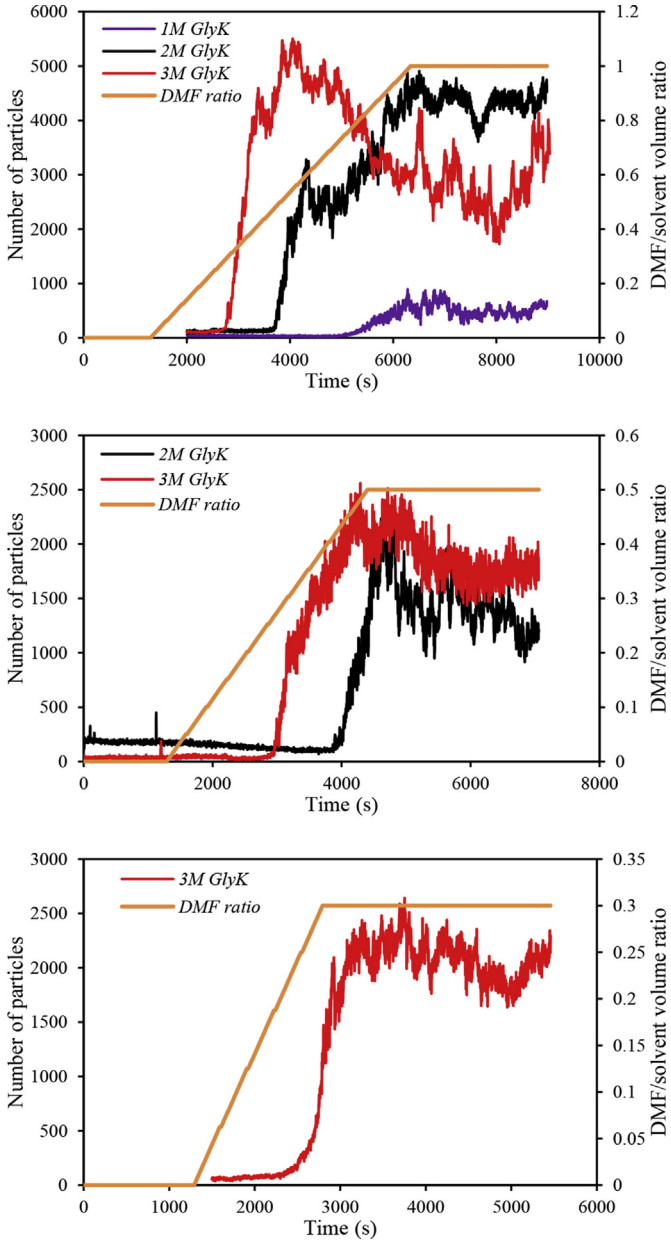

Fig. 3. Total number of precipitated solid particles and the amount of added DMF to the aqueous solution during CO_2 absorption time.

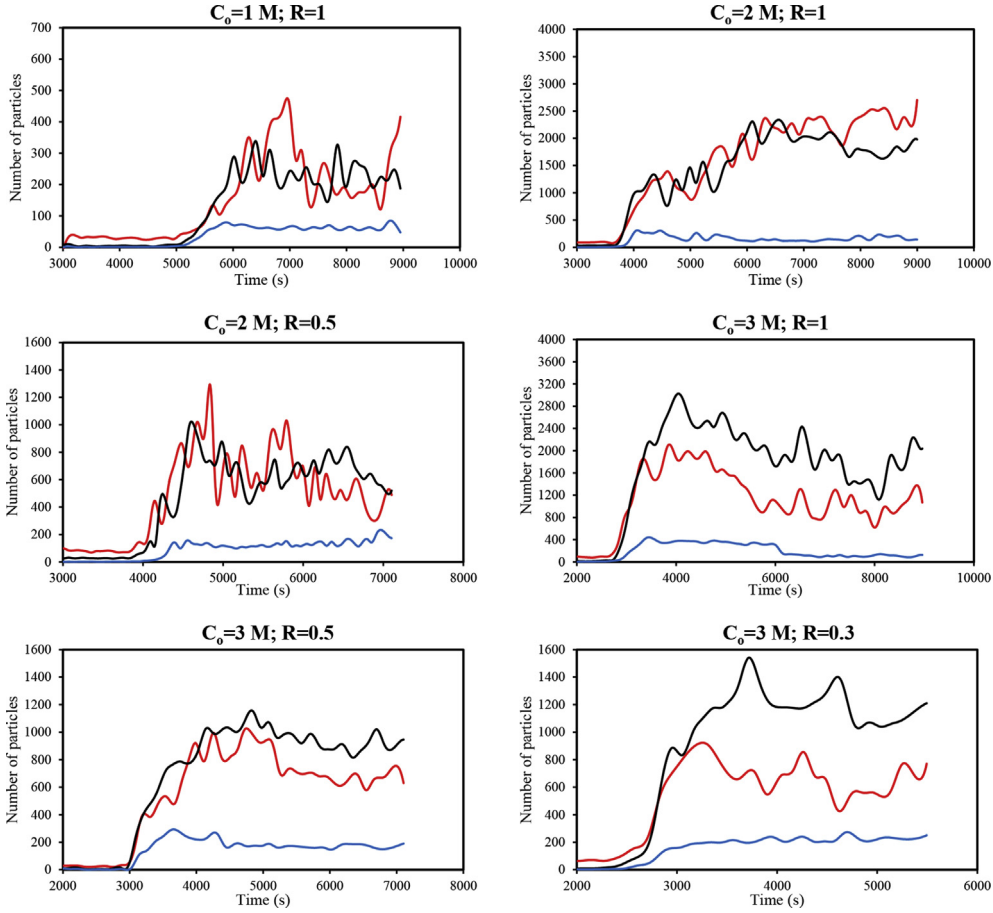

Fig. 4. The number of precipitated solid particles for different initial GlyK concentrations (C_o = 1, 2 and 3 M) and DMF to H_2O volume ratios (R = 0.3, 0.5 and 1) during CO_2 absorption. The particles with an average chord length less than 10, 10–50 and 50–150 μm are presented by red, black and blue lines, respectively.

$$n_{CO_2}^{out} = \frac{x_{CO_2}^{out}}{1 - x_{CO_2}^{out}} n_{N_2}^{out} \tag{3}$$

Using both Equation (1) and Equation (3), the rate of CO_2 absorption is calculated by:

$$Q_{CO_2} = n_{CO_2}^{in} - \frac{x_{CO_2}^{out}}{1 - x_{CO_2}^{out}} n_{N_2}^{out} \tag{4}$$

The amount of absorbed CO_2 over a given time, t, is computed by:

$$N_{CO_2} = \int_0^t Q_{CO_2} dt \tag{5}$$

Table 1
The density values of aqueous and aqueous-based GlyK-X solvents after CO_2 absorption.

Solvent	Density (mg/L)	
	Upper liquid phase	Lower liquid phase
GlyK-0	1.2867	–
GlyK-10	1.2868	–
GlyK-25	1.2930	–
GlyK-40	1.1326	1.3216
GlyK-50	1.1281	1.3604
GlyK-55	1.0894	1.4236
GlyK-60	1.0815	1.4475
GlyK-65	1.0798	1.4719

Table 2
The CO_2 absorption capacity and CO_2-containing species distribution of different aqueous and aqueous-based GlyK-X solvents.

Solvent	CO_2 loading		Carbamate		Carbonate/bicarbonate	
	Equilibrium	Dynamic (after 7 hr)				
	Mol_{CO2}/mol_{GlyK}	$Mol_{CO2}/L_{Solvent}$	$mg/g_{Solvent}$	%	$mg/g_{Solvent}$	%
GlyK-0	0.433	1.489	94.60	62.89	55.81	37.10
GlyK-10	0.435	1.492	97.33	64.42	53.75	35.58
GlyK-25	0.448	1.491	123.80	77.39	36.16	22.61
GlyK-40	0.483	1.456	152.72	48.49	162.26	51.51
GlyK-50	0.513	1.521	237.44	58.61	167.66	41.39
GlyK-55	0.539	1.621	340.41	61.98	208.81	38.02
GlyK-60	0.546	1.712	413.25	64.23	230.15	35.77
GlyK-65	0.551	1.719	426.06	65.59	223.49	34.41

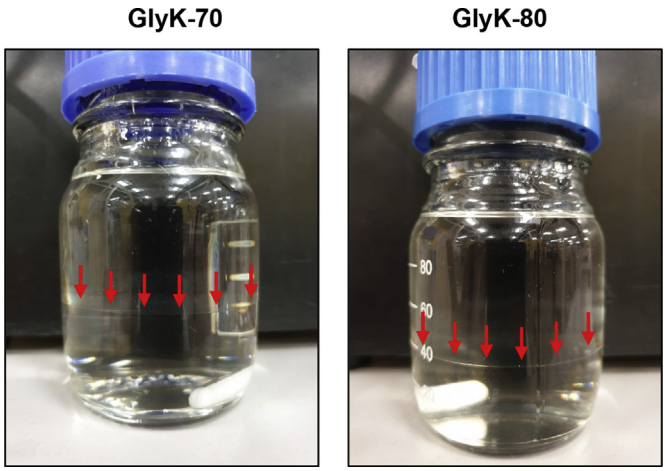

Fig. 5. The picture of aqueous-based (a) GlyK-70 and (b) GlyK-80 solvents before CO_2 absorption.

Similarly, for regeneration, the amount of desorbed CO_2 over a given time, *t*, can be obtained by:

$$N_{CO_2} = \int_0^t \frac{x_{CO_2}^{out}}{1 - x_{CO_2}^{out}} n_{N_2}^{out} dt \tag{6}$$

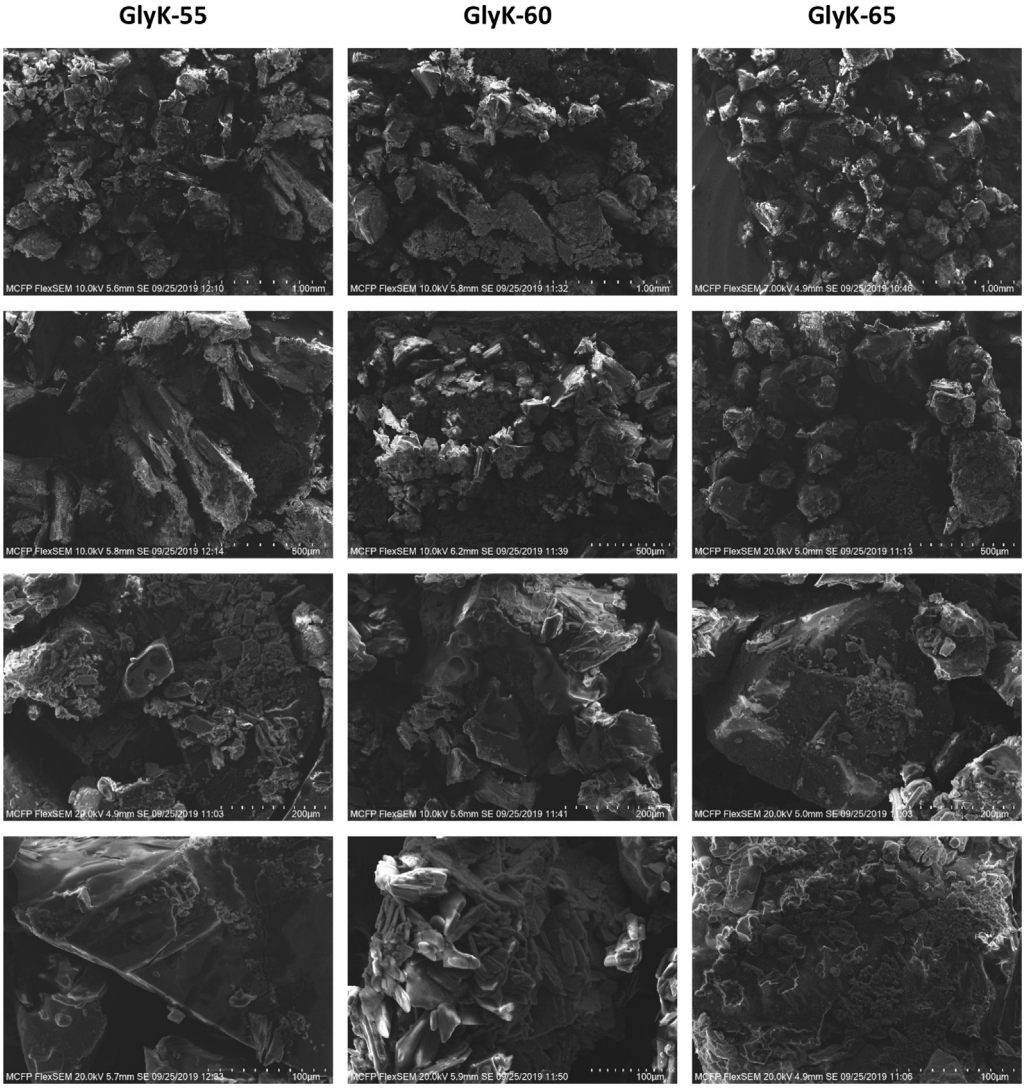

Fig. 6. The SEM analysis of solid precipitates of GlyK-55, GlyK-60 and GlyK-65 solvents at different magnifications.

2.2. CO_2 vapor-liquid equilibrium (VLE) experiments

The solubility of CO_2 in aqueous/aqueous-based solutions was measured by an in-house rig. Initially, inlet valve opened and the CO_2 container was pressurized by pure CO_2 to a desired pressure. Then, the inlet valve closed and the pressure of container was recorded (P_1). Afterward, the outlet valve was opened for 2−3 sec, while inlet valves were still closed, and pure CO_2 was injected into the equilibrium reactor. As a result, the pressure of CO_2 container decreased and reached a new pressure (P_2). Total moles of CO_2 molecules injected into the equilibrium reactor was calculated by:

$$n_{CO_2} = \frac{V_c}{RT_a}\left(\frac{P_1}{Z_1} - \frac{P_2}{Z_2}\right) \tag{7}$$

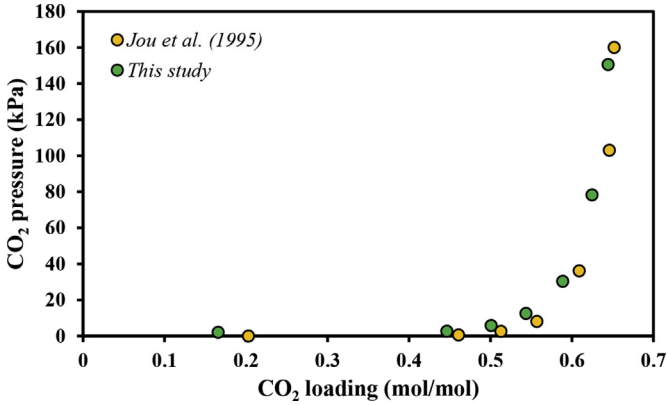

Fig. 7. The equilibrium CO_2 absorption capacity of 5 M MEA solution compared with literature data [1].

where V_c is the total volume of CO_2 container; P_1 and P_2 are the initial and final pressure of CO_2 container, respectively; Z_1 and Z_2 are gas compressibility factors associated to the initial (P_1) and final pressure (P_2) of CO_2 container; R is the universal gas constant; T_a is ambient temperature.

To calculate the compressibility factors Soave-Redlich-Kwong (SRK) was employed:

$$Z^3 - Z^2 + \left(\frac{aP - b^2P^2}{R^2T^2} - \frac{bP}{RT}\right)Z = \frac{abP^2}{R^3T^3} \tag{8}$$

All a, b and m coefficients can be calculated by:

$$a = 0.4274\frac{R^2T_c^2}{P_c}\left(1 + m\left(1 - \sqrt{T_r}\right)\right)^2 \tag{9}$$

$$b = 0.0866\frac{RT_c}{P_c} \tag{10}$$

$$m = 0.48 + 1.574\omega - 0.176\omega^2 \tag{11}$$

where T_c is the critical temperature; T_r is the reduced temperature; ω is the acentric factor.

The equilibrium pressure of CO_2 in reactor is represented as:

$$P_{CO_2} = P_R - P_V \tag{12}$$

where P_R is the reactor pressure recorded by pressure transmitter and P_V is the vapor pressure of solution.

The total number of CO_2 moles in the gaseous part of equilibrium reactor was calculated by:

$$n^g_{CO_2} = \frac{V_g P_{CO_2}}{Z_{CO_2} R T_R} \tag{13}$$

where V_g is the volume of gaseous part in the equilibrium reactor (total volume of equilibrium reactor minus the volume of loaded solution); T_R is the reactor temperature; Z_{CO_2} is the CO_2 compressibility factor at T_R and P_{CO_2}. Thus, the amount of absorbed CO_2 in liquid phase was obtained by:

$$n^{l}_{CO_2} = n_{CO_2} - n^{g}_{CO_2} \tag{14}$$

The final amount of absorbed CO_2 into the loaded solution was computed by:

$$m_{CO_2} = \frac{n^{l}_{CO_2}}{w_{sol}} \tag{15}$$

where w_{sol} is the weight of loaded solvent.

2.3. Validation and measurement accuracy

In order to validate the accuracy of VLE rig and calculation procedure (Equations (7)–(15)), the equilibrium CO_2 absorption capacity of 5 mol/L (M) MEA solution at 40 °C was compared with the previously reported data [2] and the results are illustrated in Fig. 7. As it can be seen, there is an excellent agreement between experimental data and the reported values which represent the good reliability of CO_2 VLE rig.

Acknowledgments

The authors would like to acknowledge the University of Melbourne for the Melbourne Research Scholarship, Particulate Fluids Processing Centre (PFPC) for infrastructural support and Peter Cook Centre for financial resources provided for this project.

Conflict of Interest

The authors declare that they have no known competing financial interests or personal relationships that could have appeared to influence the work reported in this paper.

References

[1] M.S. Alivand, O. Mazaheri, Y. Wu, G.W. Stevens, C.A. Scholes, K.A. Mumford, Development of aqueous-based phase change amino acid solvents for energy-efficient CO_2 capture: the role of antisolvent, Appl. Energy 256 (2019) 113911, https://doi.org/10.1016/j.apenergy.2019.113911.

[2] F.Y. Jou, A.E. Mather, F.D. Otto, The solubility of CO_2 in a 30 mass percent monoethanolamine solution, Can. J. Chem. Eng. 73 (1995) 140–147.